JOURNAL OF THEORETICAL AND APPLIED MECHANICS
50, 2, pp. 609-626, Warsaw 2012
50th Anniversary of JTAM

MICROMECHANICAL MODELLING OF DIAMOND DEBONDING IN COMPOSITE SEGMENTS

İsmail Ucun
Afyon Kocatepe University, Technical Education Faculty, Afyonkarahisar, Turkey
e-mail: iucun@aku.edu.tr

Kubilay Aslantaş
Afyon Kocatepe University, Technology Faculty, Mechanical Enginering Department, Afyonkarahisar, Turkey; e-mail: aslantas@aku.edu.tr

İ. Sedat Büyüksağiş
Afyon Kocatepe University, Engineering Faculty, Mining Engineering, Afyonkarahisar, Turkey
e-mail: sbsagis@aku.edu.tr

Süleyman Taşgetiren
Afyon Kocatepe University, Technical Education Faculty, Afyonkarahisar, Turkey
e-mail: tasgetir@aku.edu.tr

Diamond debonding in composite segments used in cutting of natural stones was investigated in this study. The finite element method was used for numerical solutions, and the problem was modelled as two dimensional. The problem was investigated under linear elastic fracture conditions. Stress intensity factors and strain energy release rates were obtained. Numerical solutions were performed for different diamond sizes and diamond heights. According to the obtained results, the most effective factor for growth of the interface crack was considered to be the tangential force acting on the diamond.

Key words: composite segment, diamond debonding, stress intensity factor, finite element method

1. Introduction

Diamond cutting discs used in cutting of natural stones are composed of two parts including the disc body and composite segments. The segments are attached by brazing on the disc body manufactured from steel. The cutting process of natural stones is performed by the diamonds within the composite matrix.

Cutting forces vary depending on the type of natural stone subjected to the cutting process, diamond concentration, diamond size and cutting parameters (Büyüksağiş and Göktan, 2005; Ersoy and Atıcı, 2004; Luo and Liao, 1993; Taşgetiren and Ucun, 2004; Ucun *et al.*, 2008). While the cutting process is performed through diamond, composite matrix holds the diamonds together. As the natural stones do not have homogenous structures, cutting forces acting on the disc during the cutting process are variable. Shock forces may cause separation of the diamond from the matrix or fracture of the diamond.

The segment is subjected to abrasive and erosive wear together with increase of the cutting volume. Height of the diamond from the matrix surface increases due to this wear and, consequently, the diamond is subjected to higher cutting forces. This may be a result of debonding of the diamond from the matrix or the diamond pull out. Failures such as fracture and flat (polish) are also seen in diamonds. Because the cutting process becomes very complicated, it is quite difficult to predict these failures. Studies about composite segments generally focus on the formation mechanism of these failures (Jennings and Wright, 1989; Luo, 1997; Luo and Liao, 1995; Ucun *et al.*, 2008; Wright and Cassapi, 1985; Yu and Xu, 2003; Zhan *et al.*, 2007). If the diamond is hard and it becomes subjected to high shock forces during the cutting process, fracture of diamonds considerably increases. When the contact temperature on the diamond becomes around 1000°C during the cutting process, some deformations may occur on the diamond surface. The surface of the diamond is flatted due to the effect of mechanical forces (Ucun, 2009). Debonding and pull out of the diamond from the composite matrix is not a desired situation among failures. The matrix is subjected to more wear by increasing of diamond pull out and therefore the forces on the segment and power consumption increase. As a result, the cutting efficiency considerably decreases. There is a chemical bond between the diamond and the composite matrix. This bond occurs during the sintering process and it is very important for effective lifecycle of the segment. The diamond may be separated from the matrix due to resulting weak interface bond and forces on diamond during the cutting process, (Karagöz and Zeren, 2001; Zeren and Karagöz, 2007). As the number of diamonds separated from the segment increases, the contact area of the matrix with the stone gets larger. This enlarged contact area causes a rise of friction and cutting forces.

In this study, diamond debonding in composite segments used as a cutting tool in natural stone industry was examined. The finite element method was used for numerical solutions and the problem was considered as two-dimensional. Cutting forces acting on the segment were experimentally determined and forces on each diamond were calculated using an analytical method.

An interface crack was defined between the diamond and the matrix. Besides, stress intensity factors and strain energy release rates were obtained depending on growth of the crack, diamond size and diamond height.

2. Diamond cutting disc

Cutting discs are generally made of alloy steels such as 75Cr1 (AISI 1075) and 80CrV2 (Tönshoff et. al, 2002) and composite segments are placed on discs using the brazing method. The segments are composite materials manufactured through the technique of powder metallurgy. Diamonds (in varying sizes and quantities) are embedded into these segments. There are two various diamond types including natural and synthetic diamonds. Synthetic diamonds are generally used in segments and they have a cubic-octahedral structure. The diamond cutting disc, composite segment and diamond used in cutting of natural stones are given in Fig. 1.

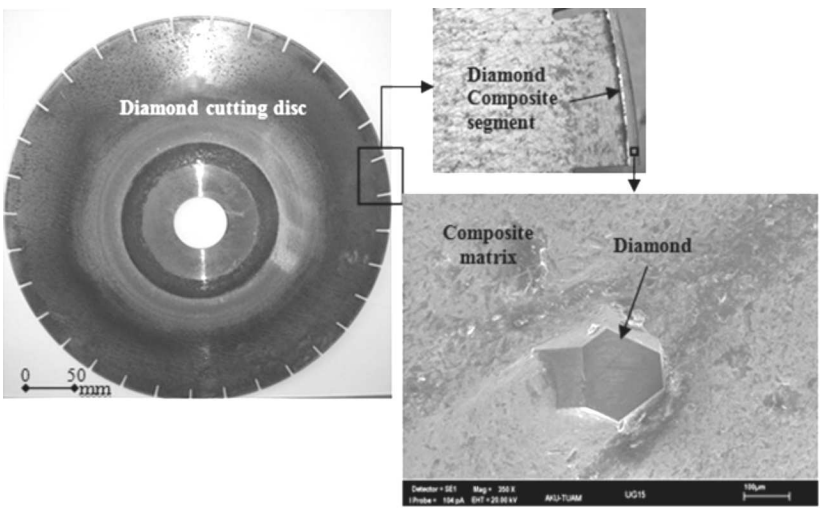

Fig. 1. Diamond cutting disc, composite segment and diamond

3. Material and methods

3.1. Calculation of stress intensity factors

The stress intensity factor is used in order to define stresses that occur in the crack region of linear elastic materials. In general, three different stress intensity factors (K_I, K_{II}, K_{III}) are defined at the edge of crack depending

on the type of loading applied to homogenous and elastic materials. Therefore, the stress intensity factor applied to the edge of crack is directly associated with the type of load applied to the material. When the problem is considered in a two-dimensional way, the opening mode (K_I) and the shear mode (K_{II}) are the two different stress intensity factors available at the edge of the crack. Although various methods are used in order to calculate K_I and K_{II} stress intensity factors that occur at the edge of the crack, the node displacement is one of the most important methods. The method gives more accurate results than other methods and, therefore, it is widely used in numerical solution methods such as the finite element method and boundary elements method. K_I and K_{II} stress intensity factors can be calculated based on the displacement values obtained from 1, 2, 3 and 4 (Fig. 2) nodes on the surface of the

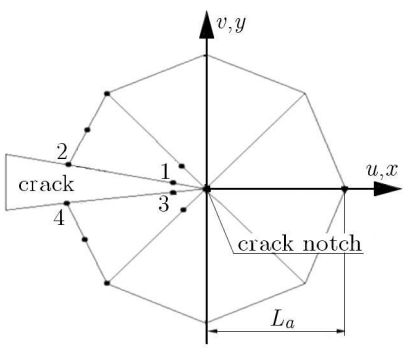

Fig. 2. Location of the nodes used to calculate the stress intensity factor

crack. The relation between the displacement values on the surface of the crack and the stress intensity factors are determined from (Aslantaş and Taşgetiren, 2004; Tan and Gao, 1990)

$$K_I = \frac{G}{\kappa+1}\sqrt{\frac{2\pi}{L_a}}[4(h_1-h_3)+(h_4-h_2)]$$
$$K_{II} = \frac{G}{\kappa+1}\sqrt{\frac{2\pi}{L_a}}[4(u_1-u_3)+(u_4-u_2)] \tag{3.1}$$

and

$$\kappa = \begin{cases} 3-4v & \text{for the plane stress} \\ \dfrac{3-v}{1+v} & \text{for the plane strain} \end{cases} \tag{3.2}$$

where, u_i and h_i are nodal displacements in the x and y directions, respectively (Fig. 2). L_a is the element length, ν is Poisson's ratio, G is the shear modulus and κ is determined for the plane stress and strain conditions.

3.2. Calculation of the strain energy release rate

The strain energy release rate is used in order to examine fracture behaviour of two different materials being interrelated or bonded. As the materials on both surfaces of the crack will be different, differences between mechanical features of both materials are expressed as α and β, and they are called the Dundurs parameters. These parameters are calculated by (Madani *et al.*, 2007)

$$\alpha = \frac{E_1' - E_2'}{E_1' + E_2'} \qquad \beta = \frac{\mu_1(1-2\nu_2) - \mu_2(1-2\nu_1)}{\mu_1(1-2\nu_2) + \mu_2(1-2\nu_1)} \tag{3.3}$$

where E_1' and E_2' are the elasticity moduli of material 1 and 2, respectively. μ and ν are the shear modulus and Poisson's ratio of the materials, respectively. The strain energy release rate as a function of crack length along the interface is explained as (Kim *et al.*, 2009; Leblond and Frelat, 2004; Madani *et al.*, 2007)

$$G_d = \frac{1}{4\cosh^2 \pi\varepsilon}\Big(\frac{1-\nu_1}{\mu_1} + \frac{1-\nu_1}{\mu_2}\Big)(K_I^2 + K_{II}^2) \tag{3.4}$$

where K_I and K_{II} are the stress intensity factors in Mod I and Mod II, ε is a function of the material constant and is explained in the following equation

$$\varepsilon = \frac{1}{2\pi} \ln \frac{1-\beta}{1+\beta} \tag{3.5}$$

3.3. Geometric model of the composite segment

A specific number of segments on the cutting disc contact with the natural stone depending on the depth of cut and these segments are subjected to cutting forces. In this study, the forces occurred during the cutting process of the granites called Blue Pearl and Nero Zimbabwe were measured through a three dimensional dynamometer (ESIT). A computer-controlled block cutting machine was used during the cutting process. The measured maximum normal and tangential forces were 610 N and 180 N, respectively (Ucun, 2009). The cutting experiments were performed with various parameters in this study. These parameters were depth of cut (a_p) 40 mm, circular velocity (V_c) 30 m/s and cutting speed (V_s) 0.6 m/min. Length of the contact with the natural stone was calculated in an analytical way depending on the depth of cut (40 mm). The number of active cutting segments and diamonds was obtained by the length of contact. The diamonds on each segment were determined using a USB microscope with a size of 250X. The normal and tangential forces on a

single diamond were determined by the following formulas (Yu *et al.*, 2006; Zhang *et al.*, 2008)

$$f_n = \frac{F_n}{A_s} \qquad f_t = \frac{F_t}{A_s} \tag{3.6}$$

where, F_t and F_n are the tangential and normal forces acting on the disc, respectively. A_s represents the number of active cutting diamonds on the composite segments. As a result of the analytical solutions, the maximum normal force acting on the diamond was obtained to be 1.135 N and the maximum tangential force was obtained to be 0.27 N.The forces were applied by distribution on a diamond as shown in Fig. 3. Geometrical features and boundary conditions of the diamond and the composite matrix used in the modelling of finite elements were given in Fig. 3.

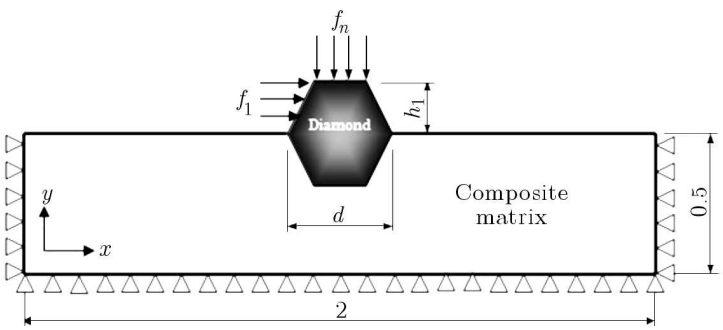

Fig. 3. Geometrical model and boundary conditions of the diamond and the matrix [mm]

Sizes of the matrix structure were selected in such a way that they would not affect the stress distribution around the diamond. Besides, image analysis software called MICROCAM was used in order to define sizes of the matrix. SEM image was obtained under cutting process conditions taken into account for determination of the two dimensional model. The image in the cross section of a diamond is shown in Fig. 4.

Indeed, the height of each diamond from the matrix h_1 and its size d are variable. For this reason, diamond size and diamond height were considered to be variable in the analyses. Geometrical features of the segment and the diamond are given in Table 1. Sizes of the diamond in the segments used in the study were taken into account as the diamond size. Sizes of the diamond within the composite segments used in the study are 40-50 US Mesh. There is a difference of 0.280 and 0.375 mm between these sizes and actual sizes of the diamond. The segment matrix and the diamonds are subjected to wear due to the forces acting on the segments. Because the matrix is subjected to a higher

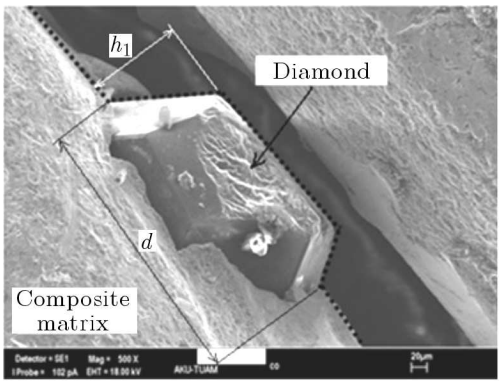

Fig. 4. Image in the cross section of the diamond

level of wear, the diamond rises to the surface. Solutions were prepared for different heights and sizes of diamond h_1 by considering the level of wear for the matrix in this study.

Table 1. Geometric properties of the diamond

Diamond heights h_1 [mm]						Diamond sizes d [mm]			
0.03	0.06	0.09	0.12	0.15	0.18	0.25	0.3	0.35	0.4

Two different materials were defined such as the diamond and the segment matrix in the finite element model. Mechanical properties of these materials are given in Table 2. Mechanical properties of the segment matrix preferred in the analyses were obtained according to EDS results.

Table 2. Mechanical properties of the segment matrix and the diamond (Hu *et al.*, 2003, 2004; Upadhyaya, 1998)

	Elasticity modulus E [GPa]	Poisson's ratio ν	Density [kg/m^3]
Diamond	1150	0.0691	3500
Segment matrix	560	0.25	8100

3.4. Finite element model of the diamond and the segment matrix

The finite element method was used to solve the problem under linear elastic fracture mechanical theory. The finite element model is done by Franc2DL

software program (Franc2DL, 2011). The finite element model of two different materials such as diamond and segment matrix is given in Fig. 5. Triangular and rectangular elements were used together in the finite element model. While triangular elements with six nodes were used in the diamond, isoparametric rectangular elements with eight nodes were preferred at the corner points of the diamond. The problem was considered in the light of two dimensional plane stress conditions. As shown in Fig. 5, a more intense mesh structure was created for the corner points, connecting the diamond and the matrix, because a considerable stress intensity occurred in the interface of the diamond and the composite matrix. As a result, possible debonding areas and cracks will start in this area. The finite element model of the problem is composed of 5346 nodes and 2259 elements.

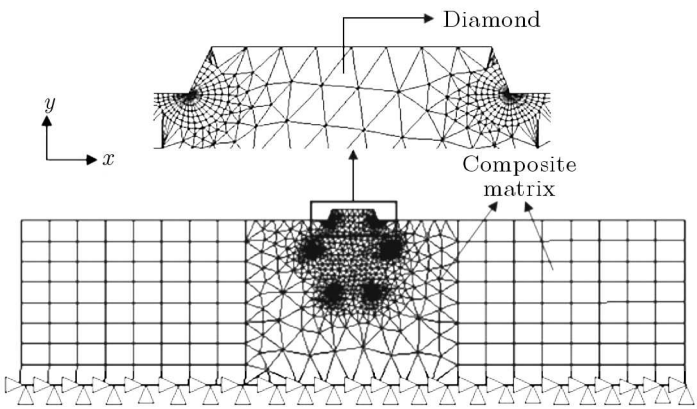

Fig. 5. Finite element model of the diamond and the composite matrix

4. Results and discussion

4.1. Stress analysis

The surface area of the segment varies depending on the depth of cut. The number of active cutting diamond also differs due to this surface area. Cutting forces acting on the segment are actually compensated by these diamonds. Due to the effect of these forces, considerable stresses occur in the diamond and the matrix that keep it intact. The equivalent stress (Von-Mises) distribution on the diamond and the matrix is shown in Fig. 6. Maximum stresses occur in the interface of the diamond and the matrix. Besides, this critical stress point is the initial point of debonding.

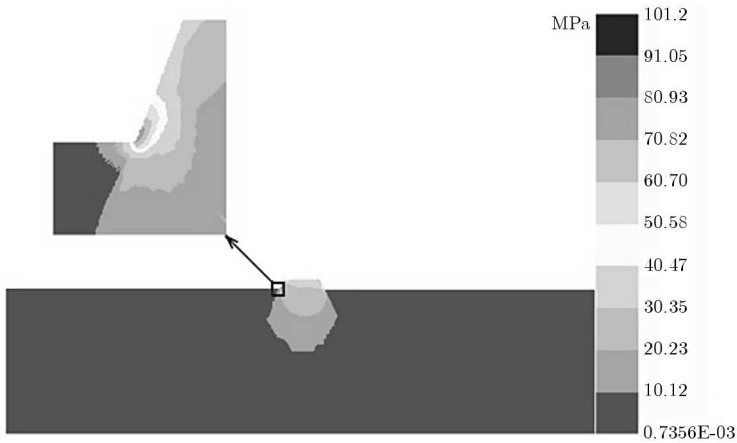

Fig. 6. Equivalent stress distribution on the diamond and the composite matrix

Variation of equivalent stresses obtained depending on the diamond size and the diamond height is given in Fig. 7. These stresses were obtained from critical areas, where the diamond and the matrix were integrated and the maximum stress integrity occurred. As the diamond size increases, it is observed that the stresses considerably decrease. Maximum stresses were obtained at 0.25 mm, where the diamond size was the lowest. As the diamond height increases, the stresses in the interface increase in a linear way and this rise occurs in two stages. Firstly, the diamond rises to the surface due to abrasive wear of the matrix (Fig. 8). Secondly, the area around the composite segment becomes hollow due to the effect of erosive wear around the diamond depending on the cutting direction (Fig. 8). For both types of wear, forces acting on the diamond and the stresses will increase. As for the resulting stresses, it is observed that the diamond height has a more important effect than that of the diamond size. While the maximum stress increases by nearly 20% with a rise in the diamond size, it increases by nearly 40% in the case of the rise in the diamond height.

In composite segments, an interface bond occurs between the diamond and the matrix. Resistance of this bond varies depending on element compounds within the matrix, element types and sintering conditions. This bond should be resistant especially against shear stresses. The bond formed between the diamond and the matrix is continuously subjected to shear stresses with the effect of tangential and normal forces, and cracks occur in the interface accordingly. Variation of shear stresses depending on the diamond size and the diamond height is given in Fig. 9. Similar to equivalent stresses, shear stresses considerably decrease with an increase in the diamond size. Minimum shear

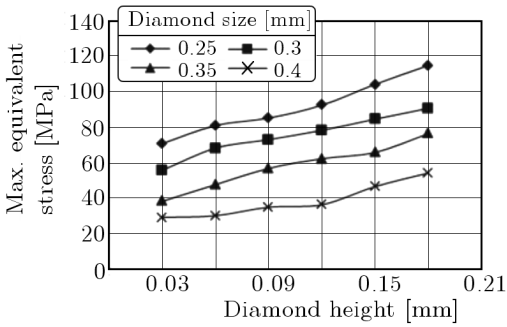

Fig. 7. Variation of the maximum equivalent stress at diamond height and size

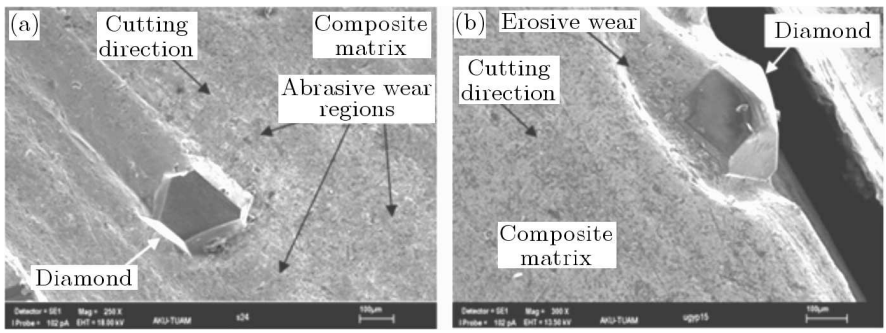

Fig. 8. Wear occurred on the diamond segment: (a) abrasive, (b) erosive

stresses were obtained when the diamond size was the maximum. In parallel with the resulting equivalent stresses, shear stresses considerably increase as the diamond size increases.

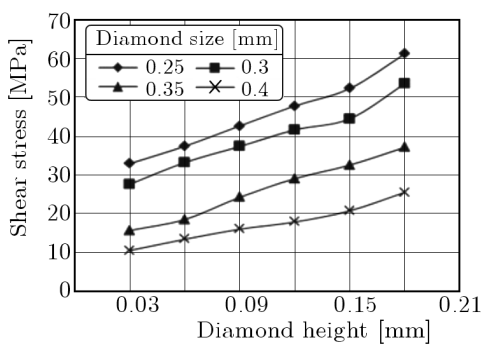

Fig. 9. Variation of shear stress at diamond height and size

4.2. Fractography

SEM (scanning electron microscopy) analysis was performed on segment surfaces after the cutting process. The observations showed that the initial point of the crack was the interface of the diamond and the matrix. It was observed that the cracks generally occurred in the interface of the diamond and the matrix in these analyses. The crack grows after a specific period of time and the diamond pulls out without completing its life.

A strong bond between the matrix and the diamond extends the lifecycle of the segment. It also minimizes the diamond pull out. However, forces acting on the segment during the cutting process may result in debonding of the diamond from the matrix. If the forces acting on the diamonds during the cutting process are not dispersed homogenously, and these forces are repetitive, compressive and tensile stresses occur in the interface of the matrix. These stresses play an important role in debonding of the diamond from the matrix. The failure mechanism in a diamond is given in Fig. 10. Before pull out of the diamond, micro cracks are formed in the critical stress point (Fig. 10a). The crack grows due to the effect of the cutting forces and the diamond debonds from the matrix and pulls out when the critical value is reached (Fig. 10c). It is suggested that debonding in the interface of the diamond and the matrix occurs based on the cutting forces. The diamond debonds from the matrix as the cutting forces are repetitive and the diamond is subjected to impact forces when it contacts with the natural stone for the first time.

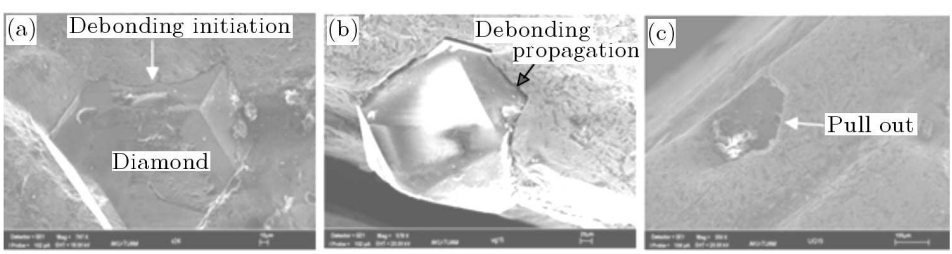

Fig. 10. Failure mechanism in the diamond

4.3. Numerical modelling of debonding

In the finite element solutions performed depending on fractography analyses, a numerical model was created for debonding that occurred between the matrix and the diamond. Debonding in the interface was defined as a crack in the finite element analysis. The crack grows with the effect of forces when the

stress intensity factor at the edge of the crack reaches the critical value. Because the problem was modelled in a two-dimensional way, two different stress intensity factors (K_I and K_{II}) were obtained at the edge of the crack. Variation of K_I with debonding length at various diamond sizes is given Fig. 11. As the length of debonding increases, K_I increases a little. After the length of crack reaches 0.05 mm, K_I stress intensity factor is subject to a sharp decline. In a sense, K_I value decreases down to the corner point of the diamond. It is fixed at very low values after this point.

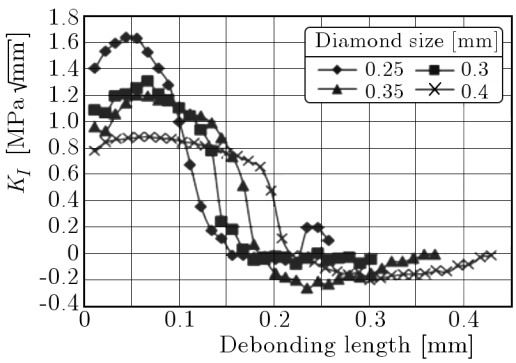

Fig. 11. Variation of K_I with debonding length

Variation of the crack length in the interface of the diamond and the matrix is given in Fig. 12. The opening mode (Mode I) is more important for debonding of the diamond up to a certain point (the 3rd state in Fig. 12). In this case, it is estimated that the tangential forces are more effective during the cutting process when compared with the normal forces. While the maximum stress intensity factor was acquired at the smallest diamond size, the minimum stress intensity factor was obtained at the largest diamond size. It is suggested that a diamond with a small size bears more risks when compared to a larger diamond in terms of debonding. After a certain length of debonding, K_I decreases to negative values. It goes up to positive values again after a certain length (see Fig. 12). This rise in K_I shows that Mode I starts to become effective again.

K_{II} value obtained in Mode II depending on different diamond sizes are given in Fig. 13. Contrary to values of K_I, K_{II} does not have any effectiveness up to a certain length of debonding. However, it was observed that through the corner point of the diamond (the 4th state in Fig. 12) the crack changed direction and became more effective when compared to Mode I. A possible debonding between the matrix and the diamond occurs with the effect of Mode II after reaching the corner point in the 3rd state (Fig. 12). In other

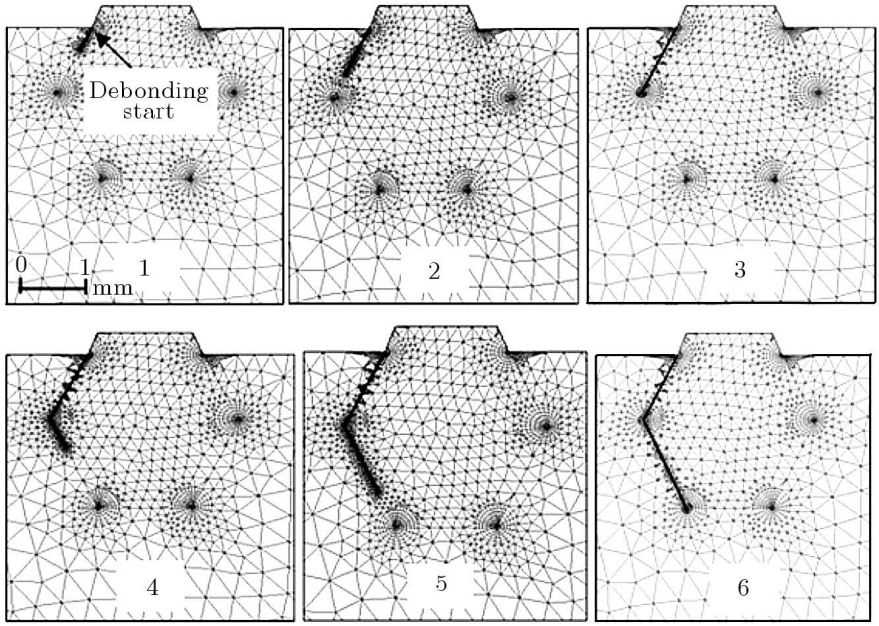

Fig. 12. Variation of debonding occurred between the diamond and the composite matrix

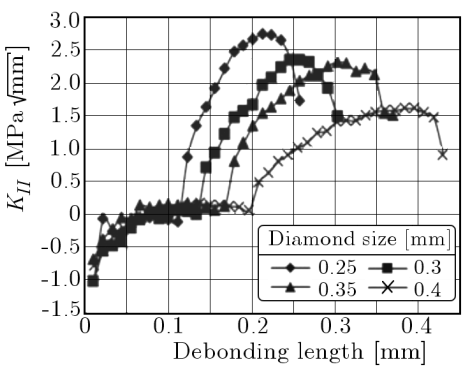

Fig. 13. Variation of K_{II} with debonding length

words, debonding occurs in the shear mode after reaching the corner point of the diamond. The opening and shear zones are shown in Fig. 14. While possible failure in the diamond zone occurs as an opening up to the 3rd state (Fig. 12), it occurs as a shear after a certain length of debonding (the 3rd to 6th states in Fig. 12).

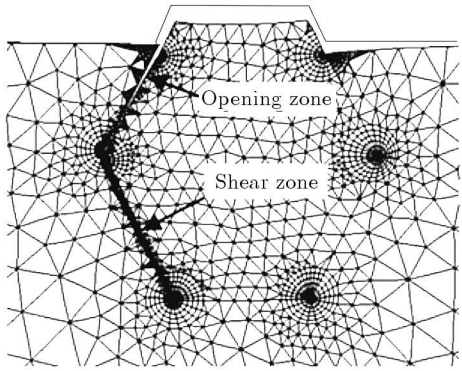

Fig. 14. Deformation region in the maximum debonding length

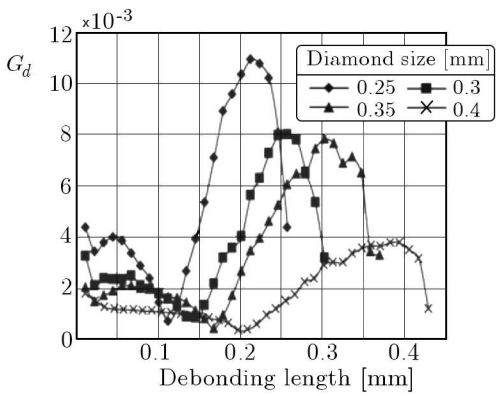

Fig. 15. Variation of the strain energy release rate with debonding length

As known, the strain energy release rate is generally taken into account for determination of possible failure for two different bonded materials. The strain energy release rates were obtained depending on the stress intensity factors obtained in the analyses (Fig. 15). While the strain energy release rate decreases a little down to a certain length of debonding for all diamond sizes, this rate considerably increases after the diamond reaches the corner point (the 3rd state in Fig. 12). This rise continues up to a certain length (the 5th state in Fig. 12). The most critical point for failure risk is the point, where the maximum strain energy release rate is achieved. As the debonding continues after this area, the strain energy release rate tends to decrease. As the strain energy release rate is low in the beginning, debonding occurs due to the effect of Mode I (opening mode). After a certain length of opening, a rapid rise in the strain energy release rate shows that Mode II (shear mode) is quite effective. A decline in the rate after the maximum value is reached indicates that the

shear effect is eliminated. Size of the diamond used within the matrix has an important effect for debonding. As the diamond size increases, the strain energy release rate considerably decreases.

5. Conclusions

In this study, debonding between the diamond and the matrix was determined in terms of experimental and theoretical methods. In the experimental study, diamond segments were investigated through SEM analysis as a result of the cutting process. Linear fracture analysis was performed using the finite element method and stress intensity factors, and strain energy release rates were obtained in the theoretical study. The following conclusions were reached as a result of this study:

- It is observed that debonding between the diamond and the matrix occurs with the effect of the cutting forces. Repetitive and variable forces acting on the diamond are considered to be the reason for debonding during the cutting process. However, it is highly possible that the diamond debonds from the matrix with the effect of scrape when the diamond segment contacts with the natural stone for the first time during the cutting process.
- Maximum equivalent and shear stresses were obtained in the corner points between the diamond and the matrix. While the diamond height increases with the matrix wear, the equivalent and the shear stresses also increase. Unlike this trend, the stresses decrease a little as the diamond size increases. Maximum stresses were obtained at small diamond sizes.
- Stress intensity factors in Mode I and Mode II were determined with the crack defined between the diamond and the matrix. Results of the fracture analysis show that the crack occurs in the opening mode (Mode I) and K_I increases with the start of debonding. However, while K_{II} values increase after reaching a certain crack length, K_I decreases. In other words, the crack grows in the shear mode (Mode II) after this length. It was observed that the diamond size had an important effect for determination of K_I and K_{II}. The stress intensity factors (K_I and K_{II}) in Mode I and Mode II increased upon a decline in the diamond size.
- The strain energy release rate explains debonding between the diamond and the matrix. The rate considerably increased upon a rise in the crack

length. The maximum strain energy release rate is the most important point in terms of failure, and this rate was obtained when the diamond had the smallest size. As the diamond size increases, the strain energy release rates decrease. It is suggested that possible failure will occur as a result of shear rather than debonding.

Acknowledgement
This study was supported by TUBITAK project (106M189 number).

References

1. Aslantaş K., Taşgetiren S., 2004, Modelling of spall formation in a plate made of austempered ductile iron having a subsurface-edge crack,*Computational Mater. Sci.*, **29**, 29-36

2. Büyüksağış I.S., Göktan R.M., 2005, Investigation of marble machining performance using an instrumented block-cutter, *J. of Mater. Process. Tech.*, **169**, 258-262

3. Denkena B., Tönshoff H.K., Friemuth T., Glatzel T., 2003, Development of advanced tools for economic and ecological grinding of granite, *Key Eng. Mater.*, **250**, 21-32

4. Ersoy A., Atici U., 2004, Performance characteristics of circular diamond saws in cutting different types of rocks, *Diamond and Related Mater.*, **13**, 22-37

5. Franc2dL, 2011, Finite element code user's manual, available from www.cfg.cornell.edu

6. Hu Y.N., Wang C.Y., Ding H.N., 2004, The mechanical performance of diamond saw blades with special structure, *Key Eng. Mater.*, **259/260**, 141-145

7. Hu Y.N., Wang C.Y., Wei X., Li Z.G., 2003, Thermodynamic analysis of diamond saw blades for dry cutting, *Key Eng. Mater.*, **250**, 233-238

8. Jennings M., Wright D., 1989, Guidelines for sawing stone, *Ind. Diamond Rev.*, **2**, 70-75

9. Karagöz ş., Zeren M., 2001, The property optimization of diamond-cutting tools with the help of microstructural characterization, *Int. J. Ref. Metals and Hard Mater.*, **19**, 1, 23-26

10. KIM J.B., SHIN B., LEE W., RHEE K.Y., 2009, Effect of virtual crack size on the crack deflection criterion at a bi-material interface under wedge loading, *Mech. Res. Communications*, **36**, 193-198

11. LEBLOND J.B., FRELAT J., 2004, Crack kinking from an initially closed, ordinary or interface crack in the presence of friction, *Eng. Fracture Mechanics*, **71**, 3, 289-307

12. LUO S.Y., 1997, Investigation of the worn surfaces of diamond sawblades in sawing granite, *J. of Mater. Process. Tech.*, **70**, 1-8

13. LUO S.Y., LIAO Y.S., 1993, Effects of diamond grain characteristics on sawblade wear, *Int. J. of Mac. Tools and Manufacture*, **3**, 2, 257-266

14. LUO S.Y., LIAO Y.S., 1995, Study of the behaviour of diamond saw-blades in stone processing, *J. of Mater. Process. Tech.*, **51**, 296-308

15. MADANI K., BELHOUARI M., BOUIADJRA B.B., SERIER B., BENGUEDIAB M., 2007, Crack deflection at an interface of alumina/metal Joint: A numerical analysis, *Computational Mater. Science*, **38**, 625-630

16. TAN C.L., GAO Y.L., 1990, Treatment of bimaterial interface crack problems using the boundary element method, *Eng. Fracture Mechanics*, **36**, 6, 919-932

17. TAŞGETIREN S., UCUN I., 2004, Determination of natural frequencies of marble cutting disc using finite element method, *Technological Research: MTED*, **1**, 4, 9-17

18. TÖNSHOFF H.K., HILLMANN-APMANN H., ASCHE J., 2002, Diamond tools in stone and civil engineering industry: Cutting principles, wear and applications, *Diamond and Rel. Material*, **11**, 736-741

19. UCUN I., 2009, *Investigation of Diamond Segments Used in Natural Stone Industry in View of Cutting Performance and Failure Analysis*, Afyon Kocatepe University, Institute for the Natural and Applied Sciences, Afyonkarahisar

20. UCUN I., ASLANTAŞ K., TAŞGETIREN S., BÜYÜKSAĞIŞ I.S., 2008, Fracture path prediction of diamond segment in a marble cutting disc, *Fatigue and Frac. of Eng. Material*, **31**, 517-525

21. UCUN I., ÇOLAKOĞLU M., TAŞGETIREN S., 2008, Crack initiation and growth in circular saw made of tool steel, *Journal of Theoretical and Applied Mechanics*, **46**, 2, 291-303

22. UPADHYAYA G.S., 1998, *Cemented Tungsten Carbides: Production, Properties and Testing*, Noyes Publications, New Jersey

23. WRIGHT D.N., CASSAPI V.B., 1985, Factors influencing stone sawability, *Ind. Diamond Rev.*, **2**, 84-87

24. YU Y.Q., XU X.P., 2003, Improvement on the performance of diamond segments for rock sawing, Part 1: Effects of segment components, *Key Eng. Mater.*, **250**, 46-53

25. Yu Y.Q., Zhang Y.F., Li Y., Xu X.P., 2006, Sawing of granite with side-slotted diamond segments, *Key Eng. Mater.*, **315/316**, 103-107

26. Zeren M., Karagöz Ş., 2007, Sintering of polycrystalline diamond cutting tools, *Materials and Design*, **28**, 3, 1055-1058

27. Zhan Y.J., Li Y., Huang H., Xu X.P., 2007, Effects of the wear characteristics of brazed diamond grits on grinding forces, *Advanced Material Research*, **24/25**, 233-238

28. Zhang G., Huang H., Xu X., 2008, Study on the wear mechanism of brazed diamond grains, *Key Eng. Mater.*, **359/360**, 58-62

Modelowanie mikromechaniczne zjawiska odpadania kryształów diamentu od kompozytowego fundamentu

Streszczenie

W pracy omówiono problem odpadania kryształów diamentu od kompozytowej matrycy narzędzi do cięcia naturalnych kamieni. Zagadnienie sformułowano dwuwymiarowo, a do uzyskania wyników symulacji numerycznych wykorzystano metodę elementów skończonych. Zjawisko badano dla warunków liniowego sprężystego pękania. Obliczono współczynniki koncentracji naprężeń oraz tempo uwalniania energii sprężystości. Symulacje przeprowadzono dla różnych wymiarów kryształów diamentu. Zgodnie z otrzymanymi rezultatami, stwierdzono, że głównym czynnikiem odpowiedzialnym za wzrost powierzchni pękania jest styczna składowa siły działającej na diament.

Manuscript received September 9, 2011; accepted for print November 16, 2011